

# Encapsulation of Hoveyda–Grubbs<sup>2nd</sup> Catalyst within Yolk–Shell Structured Silica for Olefin Metathesis

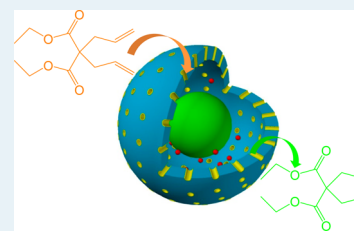
Qibiao Li, Ting Zhou, and Hengquan Yang\*

School of Chemistry and Chemical Engineering, Shanxi University, Wucheng Road 92, Taiyuan, Shanxi 030006, People's Republic of China

## Supporting Information

**ABSTRACT:** Through postreducing the pore size of a mesoporous shell, Hoveyda–Grubbs<sup>2nd</sup> catalyst was successfully encapsulated within yolk–shell structured silica, leading to a heterogeneous catalyst for olefin metathesis. Such a catalyst exhibits much higher activity than the reported encapsulated catalysts in olefin ring-closing metathesis and cross metathesis. This excellent activity can be attributed to the combination of a hollow structure in the interior and permeable mesopores in the shells. This catalyst shows good recyclability, highlighted by eight cycles of reaction. This work not only supplies an excellent heterogeneous olefin metathesis catalyst but also demonstrates that yolk–shell structured silica materials can be used as an innovative scaffold to encapsulate homogeneous catalysts.

**KEYWORDS:** olefin metathesis, Hoveyda–Grubbs<sup>2nd</sup> catalyst, encapsulation, yolk–shell structure, mesoporous silica



## INTRODUCTION

Ru complex catalyzed olefin metathesis has become an important tool to generate new C=C bonds. The commercial availability of Hoveyda–Grubbs<sup>2nd</sup> catalysts and their good functional group tolerance ability and mild reaction conditions make this reaction accessible to a variety of olefins, even including polymeric materials and natural products.<sup>1–4</sup> However, these well-established elegant homogeneous catalysts still suffer from difficulty in catalyst separation and recycling, which constitutes a serious obstacle to large-scale industrial applications. To circumvent this obstacle, many attempts have been made to immobilize these Ru complex catalysts on insoluble solid materials through covalent linkage, electrostatic adsorption, and encapsulation, thereby achieving recoverable catalysts.<sup>5–21</sup> Alternatively, water-soluble Ru complexes and light switch tagged Ru complexes were developed with the aim of recycling the homogeneous catalyst by virtue of biphasic systems.<sup>22–25</sup> Although encouraging and interesting results have been obtained, these recyclable catalysts either require relatively complicated preparation procedures or show significantly decreased activity in comparison to their homogeneous counterparts. In this context, highly active and recyclable catalysts that can be prepared by a simple procedure are desirable.

Among the various methods to transfer homogeneous to heterogeneous catalysts, encapsulation may be preferable because it does not require chemical modification of the initially perfect catalyst structure on which the catalytic performances strongly depend, and negative effects caused by supports can be decreased owing to the absence of a direct covalent linkage or electrostatic interaction with supports. Along this line, we have recently developed an efficient method to encapsulate homogeneous catalysts: namely, spatially confining metal complexes in the nanocages of mesoporous

silica by reducing the pore entrance size. With this approach, our group and other groups succeeded in the encapsulation of metal complexes such as Co(salen), Cr(salen), VO(salen), Mn(salen), Ru-TsDPEN, and Hoveyda–Grubbs<sup>2nd</sup> catalyst in the nanocages of the mesoporous materials SBA-16 and SBA-1.<sup>26–32</sup> These encapsulated catalysts showed good activity, moderate to excellent recyclability, and interesting confinement effects. Although our series of works sufficiently demonstrated that the obtained catalytic performances are strongly dependent on the support structures, our method is still limited to the use of mesoporous cage-like SBA-16 and SBA-1 as supports. Accordingly, the exploration of new supports for encapsulating homogeneous catalysts so as to achieve a more efficient heterogeneous catalyst is desired.

Yolk–shell structured mesoporous materials containing a void space between the core and the outer shell of the material are emerging as an interesting family of new hollow nanoarchitectures.<sup>33–48</sup> The enclosed void space is expected to be useful for accommodating various guest molecules or nanoparticles, while the mesoporous shell allows reactant molecules to permeate the shell to enter the void space. Such a nanoarchitecture is entirely different from the previously used cage-like mesoporous materials. Furthermore, the dimensions of the void space and shell pore size are both tunable. Despite these features that might lead to more efficient heterogeneous catalysts, there have been no reports on encapsulation of homogeneous catalysts within yolk–shell structured silica to date.

Herein, we first demonstrate the encapsulation of Hoveyda–Grubbs<sup>2nd</sup> catalysts within yolk–shell structured mesoporous

Received: October 7, 2014

Revised: February 3, 2015

Published: February 25, 2015

silica by reducing the shell pore size through a silylation method. The encapsulated Hoveyda–Grubbs<sup>2nd</sup> catalyst shows much higher activity and recyclability in comparison to its analogous heterogeneous catalysts. Moreover, this work demonstrates that yolk–shell structured materials can be used as an innovative scaffold to encapsulate homogeneous catalysts.

## EXPERIMENTAL PROCEDURES

**Chemicals.** Tetraethyl orthosilicate (TEOS, AR) was purchased from Alfa Aesar. Ammonia solution (25–28%), dodecyltrimethylammonium bromide (DTAB, AR), ethanol, acetone (AR), toluene (AR), hexane (AR), pyridine (AR), dichloromethane (AR), and sodium carbonate (AR) were purchased from Sinopharm Chemical Reagent Co. (Shanghai, China). Hoveyda–Grubbs<sup>2nd</sup> catalyst (CAS No. 301224-40-8), dichlorodiphenylsilane (>95%), and the substrates were purchased from Aldrich Co. Deionized water was used in all experiments.

**Preparation of Yolk–Shell Structured Mesoporous Silica (Y-S).** SiO<sub>2</sub> nanospheres were synthesized according to a modified Stöber method.<sup>49</sup> A 16 mL portion of aqueous ammonia, 200 mL of ethanol, and 12.2 mL of deionized water were mixed. After the mixture was stirred for 0.5 h (1500 rpm), 12.4 mL of TEOS was added dropwise. Further stirring for 12 h at room temperature resulted in a white silica colloidal suspension. The silica particles were collected through centrifugal separation, then washed with deionized water (30 mL × 6) and ethanol (20 mL × 2), and finally dried at 60 °C for 4 h in air, leading to SiO<sub>2</sub> nanospheres.

The above silica nanospheres (1.0 g) were dispersed in 500 mL of deionized water by ultrasonication. DTAB (1.27 g), ethanol (300 mL), and concentrated ammonia solution (5.5 mL) were added to this suspension. After the mixture was stirred for 0.5 h at room temperature, 2.35 g of TEOS was added dropwise. After further stirring for 7 h, the solid was collected by centrifugation, washed with deionized water and ethanol, and dried at room temperature. The resultant solid powder was dispersed in 200 mL of water containing 4.24 g of Na<sub>2</sub>CO<sub>3</sub> by ultrasonication. After the mixture was stirred for 4 h at 50 °C, the solid was isolated by centrifugation and thoroughly washed with deionized water (60 mL × 6) and ethanol (20 mL × 2). In addition, the obtained solid was subjected to calcination to remove the template DTAB (the temperature was raised from room temperature to 550 °C at a rate of 1 °C/min and further maintained for 5 h in an air atmosphere). The finally obtained yolk–shell material was denoted as Y-S. For comparison, Y-S materials with thinner and thicker shells were also prepared by only changing the amount of TEOS used for shell growth. TOES portions of 1.76 and 2.94 g were used for the former and latter, respectively. In parallel, the completely hollow mesoporous silica was prepared by only prolonging the etching time to 12 h.

**Encapsulation of Hoveyda–Grubbs<sup>2nd</sup> Catalyst.** A 1.0 g portion of Y-S was dispersed in a mixture of 10 mL of toluene containing 0.02 g of Hoveyda–Grubbs<sup>2nd</sup> catalyst. After the mixture was stirred for 4 h at room temperature under an N<sub>2</sub> atmosphere, the solid was dried under vacuum. The obtained solid was dispersed in a mixture of 8.0 mL of dry hexane containing 0.38 g of dichlorodiphenylsilane and 0.018 g of pyridine. After the mixture was stirred for 6 h at 35 °C under an N<sub>2</sub> atmosphere, the resultant solid was collected through centrifugal separation, repeatedly washed with dichloromethane (4.5 mL × 6), and dried under vacuum, eventually leading to

the Ru@Y-S catalysts. All used dichloromethane solutions were collected and analyzed with a UV/vis spectrophotometer to estimate the residual amount of Hoveyda–Grubbs<sup>2nd</sup> catalyst. On the basis of the difference between the initially used amount and the residual amount, the Hoveyda–Grubbs<sup>2nd</sup> catalyst loading was determined as  $9.57 \times 10^{-3}$  mmol g<sup>-1</sup>. This result is in agreement with the ICP-AES results.

**Catalyst Characterization.** TEM micrographs were taken with a JEM-2000EX transmission electron microscope (operated at 120 kV). Small-angle X-ray powder diffraction analysis was performed on a Rigaku D/max rA X-ray diffractometer (at 40 kV and 30 mA with Cu K $\alpha$  radiation). N<sub>2</sub> physical adsorption was performed on a Micromeritics ASAP 2020 volumetric adsorption analyzer (before the measurements, samples were outgassed at 398 K for 8 h). The BET specific surface areas were evaluated from data in the relative pressure range from 0.05 to 0.25. The total pore volume was estimated from the amount adsorbed at the highest P/P<sub>0</sub> (above 0.99). UV/vis spectra were recorded on a JASCO V-550 UV/vis spectrophotometer. Diffuse-reflectance UV/vis spectra were also recorded on a CARY 300 spectrophotometer (Varian Co.). <sup>13</sup>C CP-MAS NMR spectra were recorded on an Infinity plus 300 MHz spectrometer (75.4 MHz resonant frequency, 4 kHz spin rate, 4 s pulse delay, 1.0 ms contact time, hexamethylbenzene as a reference compound). Thermal gravimetric (TG) experiments were carried out with a NETZSCH TG analyzer (Germany) under a nitrogen atmosphere from room temperature to 950 °C with a heating rate of 10 °C/min. The leached Ru was analyzed by inductively coupled plasma-atomic emission spectrometry (ICP-AES, AtomScan16, TJA Co.). GC analysis was conducted on an Agilent 7890A instrument.

**Catalysis Reaction and Catalyst Recycling.** A 1 mL portion of dry dichloromethane, 0.1 mmol of substrate, and a given amount of the solid catalyst containing 0.001 mmol of Ru were placed in a tube. This tube was sealed under an N<sub>2</sub> atmosphere for reaction at given temperature. At the end of the reaction, the liquid was withdrawn after centrifugation and diluted with dichloromethane for GC analysis. The collected solid catalyst was washed thoroughly with dichloromethane (2 mL × 3) and dried under vacuum for the next reaction cycle.

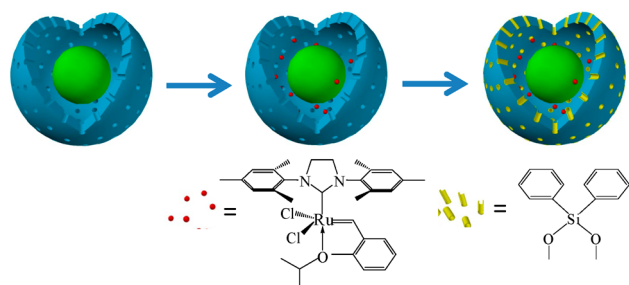
**Filtrate Activity Test.** A 2 mL portion of dry dichloromethane, 0.2 mmol of diethyl diallyl malonate, and a given amount of solid catalyst (containing 0.002 mmol of Ru complex) were mixed. The mixture was stirred at 25 °C under an N<sub>2</sub> atmosphere. After 15 min, the reaction was stopped. After rapid centrifugation, half of the filtrate (without solid catalyst) was transferred to a new tube and continuously stirred at 25 °C under an N<sub>2</sub> atmosphere. The other half of the filtrate containing the solid catalyst was also continuously stirred under the same conditions. These two reactions were monitored by GC every 30 min.

## RESULTS AND DISCUSSION

**Catalyst Preparation and Characterization.** On the basis of the optimized geometries, the three-dimensional size of Hoveyda–Grubbs<sup>2nd</sup> catalyst is estimated to be 1.76 nm × 1.35 nm × 1.05 nm.<sup>30</sup> To allow this complex to pass through the shell and enter the interior of yolk–shell structured silica, we synthesized yolk–shell mesoporous silica material with a shell pore size of 2.2 nm (the N<sub>2</sub> sorption isotherms and pore size distribution calculated by the DFT method are provided in Figure S1 in the Supporting Information), slightly larger than

the size of the complex. The procedure for encapsulating Hoveyda–Grubbs<sup>2nd</sup> catalyst within yolk–shell structured silica consists of two steps; the diagram is shown in Scheme 1. The

### Scheme 1. Process for Encapsulating Hoveyda–Grubbs<sup>2nd</sup> Catalyst within a Yolk–Shell Structured Silica through Silylation



yolk–shell structured silica was first impregnated with toluene solution containing Hoveyda–Grubbs<sup>2nd</sup> catalyst, allowing Ru complexes to enter the interior of yolk–shell structured silica. In the following step, the shell pores of yolk–shell silica were reduced through silylation of dichlorodiphenylsilane. After thorough washing with dichloromethane to remove Hoveyda–Grubbs<sup>2nd</sup> catalyst located on the external surface, the Ru@Y-S catalyst was obtained. The whole preparation process is very simple in comparison to other immobilized Hoveyda–Grubbs<sup>2nd</sup> catalysts. Since the molecular size of grafted diphenylsilane is estimated as 0.6 nm, the pore size of yolk–shell structured silica was estimated as 1.0 nm ( $2.2 - 2 \times 0.6$ ), which is smaller than the size of the Hoveyda–Grubbs<sup>2nd</sup> catalyst molecule. As a result, Hoveyda–Grubbs<sup>2nd</sup> catalyst was spatially confined in the void space of yolk–shell silica. The

amount of Ru complex entrapped inside the yolk–shell structured material is about  $9.57 \times 10^{-3} \text{ mmol g}^{-1}$ . About 30% of the initially added Ru complex was encapsulated within the yolk–shell silica. In contrast, it was found that only 9% and 15% of the initially added Ru complex were encapsulated within core–shell silica (without etching) and the completely hollow silica, respectively (Table S1 and Figure S2 in the Supporting Information). These comparisons may suggest that the internal cavity is helpful in accommodating the metal complex and the core of the yolk–shell structure serves as a support to adsorb the metal complex to prevent it from escaping during silylation. Moreover, only 15% of the initially added Ru complex was retained in the yolk–shell materials without silylation modification (most of the Ru complexes were observed to be removed during the course of washing with polar solvent). This set of comparisons confirms that our encapsulation protocol with the yolk–shell structure mesoporous silica is effective at trapping Hoveyda–Grubbs<sup>2nd</sup> catalyst.

The structures of the Ru@Y-S catalyst were characterized with transmission electron microscopy (TEM), X-ray diffraction (XRD), and N<sub>2</sub> physical sorption. As the TEM image shows (Figure 1a), the Ru@Y-S catalyst consists of monodisperse yolk–shell structured spherical particles. There is a void space between the shell and core, which is a typical yolk–shell structure. The diameter of the whole yolk–shell silica is ca. 540 nm. The shell thickness and core diameter are ca. 70 and 320 nm, respectively. From the high-resolution TEM image (Figure 1b), one can clearly see that the ordered mesopores are present on the shell of Ru@Y-S and their diameters are ca. 2 nm. Interestingly, the mesopores in the shell are radially aligned (oriented to the outer shell boundary). The low-angle XRD pattern of Ru@Y-S displays a broad diffraction peak at  $2\theta = 2.9^\circ$  (Figure 1c), indicating the mesopore

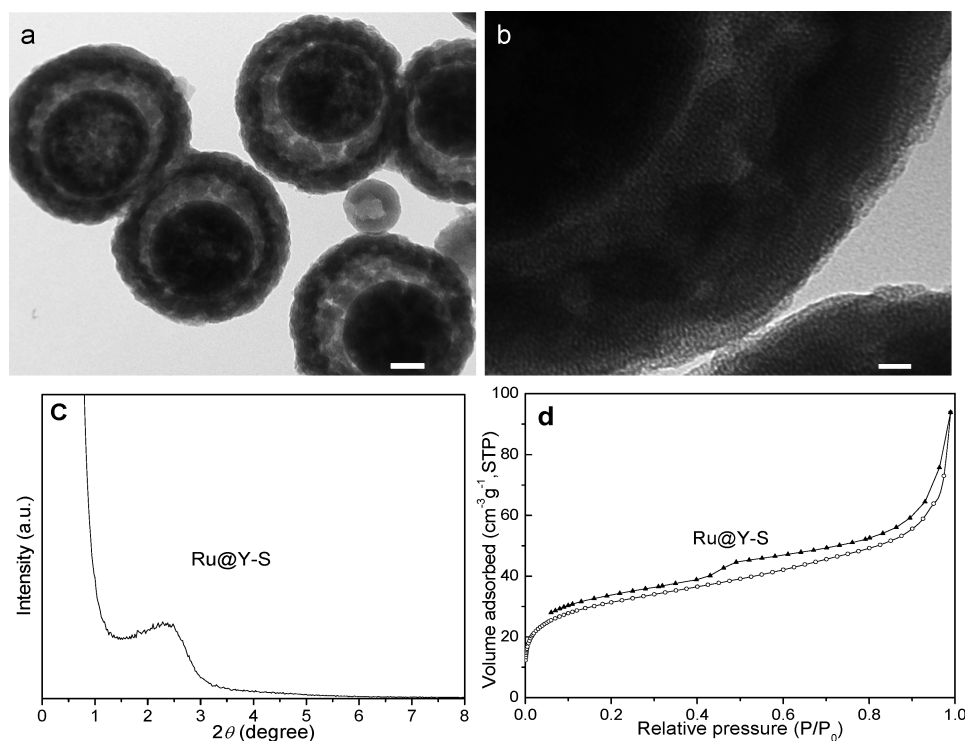


**Figure 1.** Structural characterization of the Ru@Y-S catalyst: (a) TEM image, less magnified (the scale bar is 100 nm); (b) TEM image, more magnified (the scale bar is 20 nm); (c) XRD pattern; (d) N<sub>2</sub> sorption isotherm.



structures in the shell. The N<sub>2</sub> sorption isotherms of Ru@Y-S exhibit a type IV isotherm (Figure 1d). Notably, a pronounced hysteresis with delayed capillary evaporation at a relative pressure of 0.43–0.99 was observed. This feature indicates that there is a void structure,<sup>41,50</sup> which is in good agreement with the TEM observations. In comparison with Y-S, the surface area and pore volume are progressively decreased from 401 to 129 m<sup>2</sup> g<sup>-1</sup> and from 0.26 to 0.15 cm<sup>3</sup> g<sup>-1</sup>, respectively. Such changes are caused by the silylation modification and location of Hoveyda–Grubbs<sup>2nd</sup> catalyst inside the interior void.

The composition of the Ru@Y-S catalyst was characterized by a diffusion reflectance UV–vis spectrum. The solid catalyst exhibits a remarkable absorbance band at 377 nm (Figure 2),

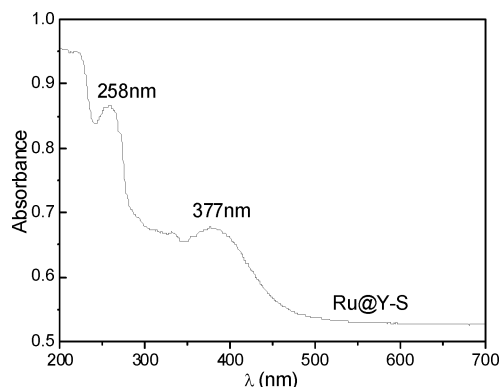


**Figure 2.** Diffusion reflectance UV/vis spectrum of the Ru@Y-S catalyst.

which is the characteristic absorbance of Hoveyda–Grubbs<sup>2nd</sup> catalyst (as shown in Figure S3 in the Supporting Information). This finding confirms that Hoveyda–Grubbs<sup>2nd</sup> catalyst was successfully encapsulated within the yolk–shell structured silica. The <sup>13</sup>C cross-polarization magic-angle spinning (CP-MAS) NMR spectrum of the Ru@Y-S catalyst exhibits strong signals at 128 and 134 ppm, which are attributed to the benzene ring. The signals for the Ru complex such as those of the isopropyl groups (at 15–30 ppm) were not detected because the loading of the Ru complex was relatively low (Figure S4 in the Supporting Information). The thermal gravimetric (TG) curves are provided in Figure S5 in the Supporting Information. The yolk–shell structured silica is subjected to 2.0% weight loss in the range 100–800 °C, which is due to the Si–OH condensation accompanied by dehydration. For diphenylsilane modified yolk–shell structured silica without encapsulation of Hoveyda–Grubbs<sup>2nd</sup> catalyst, there is significantly increased weight loss from 490 to 800 °C in comparison to the bare yolk–shell silica, which is attributed to diphenyl moiety decomposition. Notably, different from the diphenylsilane modified yolk–shell silica without encapsulation of Hoveyda–Grubbs<sup>2nd</sup> catalyst, the Ru@Y-S catalyst exhibits two steps of weight loss curve in the range 490–800 °C. There is a relatively sharp loss from 490 to 530 °C, followed by a slow loss from 530 to 800 °C. The former sharp loss may be caused mainly by the decomposition of Hoveyda–Grubbs<sup>2nd</sup> catalyst, while the latter is mainly due to diphenyl moiety decomposition.

**Catalytic Activity Evaluation.** The Ru@Y-S catalyst was first examined with ring-closing metathesis (RCM) of diethyl diallylmalonate with 1 mol % Ru (with respect to substrate) at room temperature, using dichloromethane as solvent. The

kinetic profile was monitored with GC, as shown in Figure S6 in the Supporting Information. The conversion of diethyl diallylmalonate increased with the extension of time and reached 82% within 105 min and 96% within 180 min. Under the same conditions, the reaction rate over the Ru@Y-S catalyst is slower than that over the homogeneous Hoveyda–Grubbs<sup>2nd</sup> catalyst. The decreased reaction rate may be attributed to the diffusion resistance of the mesoporous shell. However, the reaction rate over Ru@Y-S is much higher than those obtained with the Hoveyda–Grubbs<sup>2nd</sup> catalyst encapsulated in core–shell structured silica (62%) and hollow mesoporous silica (87%) (Table S1 in the Supporting Information). To further clarify the diffusion effects, we compared its reaction rate with those of the Ru@Y-S catalyst with thinner shell and thicker shell (Figure S7 in the Supporting Information). The reaction rate slightly increases with a decrease in the shell thickness, which confirms that there actually is diffusion resistance for the yolk–shell catalysts. However, the reaction rate over the Ru@Y-S catalyst is much faster than that of our previously reported Ru@SBA-1 catalyst<sup>32</sup> (50% conversion within 105 min; Figure S6), which is the Hoveyda–Grubbs<sup>2nd</sup> catalyst encapsulated with the mesoporous material SBA-1.

The catalytic performances of Ru@Y-S were examined with RCM of other dienes. The results are summarized in Table 1.

**Table 1.** RCM Reactions of Various Dienes over the Ru@Y-S Catalyst<sup>a</sup>

Entry	Substrates	Products	Time/h	Conv.% <sup>b</sup>
1			3	96
2			3	97
3			4	99
4			4	89
5			3	99
6			4	90
7			5	99

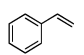
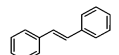
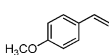
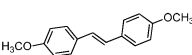
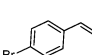
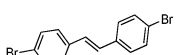
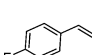
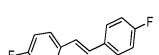
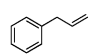
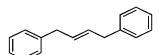
<sup>a</sup>Reaction conditions: 0.1 mmol of substrate (0.1 mmol mL<sup>-1</sup>), 1 mol % of Ru with respect to substrate, 1 mL of dichloromethane as solvent, 25 °C. <sup>b</sup>Determined with GC.

The conversion of diethyl diallylmalonate reached 96% within 3 h (entry 1). Diallyl acetylacetonate was transformed to a cyclic product with excellent conversion (97%, entry 2). For diallyl sulfonamide (entry 3), a conversion of 99% was obtained within 4 h. The cyclization of *N,N*-diallylbenzamide afforded a conversion of 89% within 4 h (entry 4). Diallyl ether was converted to a cyclic product with a 99% conversion within 3 h (entry 5). 1,7-Octadiene was transformed to cyclohexene with a 90% conversion (entry 6). Bis(4-butenyl)-substituted diethyl malonate could be also smoothly cyclized with a conversion of 99% within 5 h (entry 7). In these investigated reactants, the Ru@Y-S catalyst showed much higher activity than Ru@SBA-1

(the comparisons of their TOFs are shown in Table S2 in the Supporting Information). These results demonstrate the superiority of yolk-shell structured materials over mesoporous materials such as SBA-1.<sup>31,32</sup> The excellent reactivity of Ru@Y-S should be related to the unique yolk-shell mesoporous structure. Due to the presence of a void space in the interior of the support, the reactant molecules can transport more quickly inside the catalyst particle in comparison to the case for the cage-like mesoporous material SBA-1. Moreover, the radially aligned mesopores in the shell are favorable for reactant molecules to permeate the shell to directly access the Ru complexes.

The Ru@Y-S catalyst also showed good activity toward olefin cross-metathesis (CM). The CM over the Ru@Y-S catalyst was also conducted at 35 °C in the presence of 2.5 mol % of Ru, also using dichloromethane as solvent. The results are summarized in Table 2. Within 5 h, styrene was smoothly

**Table 2. CM Reactions of Various Substrates over the Ru@Y-S Catalyst<sup>a</sup>**

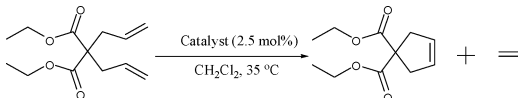
Entry	Substrates	Products	Time/h	Conv.% <sup>b</sup>
1			5	99
2			5	86
3			5	74
4			5	95
5			5	96

<sup>a</sup>Reaction conditions: 0.1 mmol of substrate (0.1 mmol mL<sup>-1</sup>), 2.5 mol % of Ru with respect to substrate, 1 mL of dichloromethane as solvent, 35 °C. <sup>b</sup>Determined with GC.

converted to 1,2-diphenylethene with a conversion of 99% (entry 1); methoxy-substituted styrene gave a conversion of 86% (entry 2). For 4-bromostyrene and 4-fluorostyrene, the conversions were up to 74% and 95%, respectively (entries 3 and 4); the conversion of allylbenzene reached as high as 96% (entry 5). The experiments demonstrate a functional group tolerance for the Ru@Y-S catalyst.

The recyclability of the Ru@Y-S catalyst was tested with consecutive RCM of the diethyl diallylmalonate reaction. The results are given in Table 3. The fresh solid Ru@Y-S catalyst

**Table 3. Recycling Results of RCM over the Ru@Y-S Catalyst<sup>a</sup>**

								
reacn cycle	1	2	3	4	5	6	7	8
time/h	2	2	2	2	2	3	5	7
conversn/%	99	96	91	87	66	69	64	50

<sup>a</sup>Reaction conditions: 0.1 mmol of diethyl diallylmalonate (0.1 mmol mL<sup>-1</sup>), 2.5 mol % of Ru with respect to substrate, 1 mL of dichloromethane as solvent, 35 °C. <sup>b</sup>Determined with GC.

gave 99% conversion of diethyl diallylmalonate within 2 h at 35 °C (using 2.5 mol % Ru with respect to substrate). After the first reaction cycle, the catalyst could be recovered by centrifugation. After being washed with dichloromethane (2 mL × 3) and dried under vacuum, the recovered catalyst was directly used for the next reaction cycle. In the second and third reaction cycles, the conversion reached 96% and 91%, respectively. Although the catalytic activity began to decrease from the fourth reaction cycle on, 87% and 66% of conversions were still obtained in the fourth and fifth reaction cycles, respectively. To obtain good conversions, the reaction time was prolonged in the following reaction cycles. For the eighth reaction cycle, 50% conversion was still achieved. The Ru contents in the filtrate of the first reaction cycle and the eighth reaction cycle were determined as ca. 4 and 1 ppm, respectively. These results probably indicate that the deactivation of our catalyst may be mainly due to a change in the Hoveyda-Grubbs<sup>2nd</sup> catalyst itself such as isomerization or dimerization instead of Ru complex leaching, which is preliminarily supported by the catalyst color change from green to gray.<sup>51,52</sup> Under the same conditions, for the Ru complex-loaded yolk-shell structured silica without silylation as catalyst, the first reaction cycle gave only 72% conversion of diethyl diallylmalonate (Table S3 in the Supporting Information); in the second and third reaction cycles, the conversion rapidly declined to 27% and 5%, respectively. These remarkable contrasts indicate that reducing pore size through silylation is crucial in preventing Ru complex leaching from the support.

In order to check the heterogeneous nature of reaction in the presence of the Ru@Y-S catalyst, the activity of the filtrate was examined. When the reaction proceeded for a period of 15 min, the RCM reaction of diethyl diallylmalonate was stopped. After rapid centrifugation, one portion of the upper filtrate (without solid catalyst) was immediately transferred into another reaction vessel and further stirred as in the standard RCM reaction procedure. The residual mixture containing the Ru@Y-S catalyst was also continuously stirred for further reaction. Their conversions versus time over the Ru@Y-S catalyst and in the filtrate were monitored by GC (Figure 3). In the presence of the Ru@Y-S catalyst the conversion increases with time, while the conversion in the filtrate does not show any increase. These results are in good agreement with the aforementioned determination results of the Ru contents in the filtrate. These

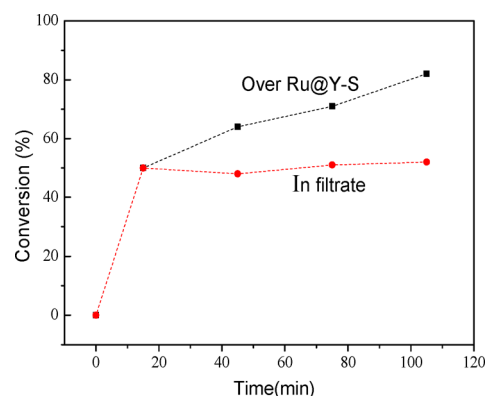


**Figure 3.** Profiles of the conversions versus time for the RCM of diethyl diallylmalonate over the Ru@Y-S catalyst and in the filtrate (1 mol % Ru with respect to substrate, dichloromethane as solvent, 25 °C).

results also revealed that the conversion indeed contributed to the solid catalyst instead of the leached Ru complex in the filtrate, further confirming the effectiveness of our encapsulation protocol.

## CONCLUSIONS

The Hoveyda–Grubbs<sup>2nd</sup> catalyst was successfully encapsulated within yolk–shell structured silica by postreducing the pore size through silylation. The obtained Ru@Y-S catalyst exhibited excellent activity and recyclability in the RCM and CM of various olefins. Its activity proved much higher than that of the analogous encapsulated Hoveyda–Grubbs<sup>2nd</sup> catalyst. The high activity could be attributed to the unique yolk–shell mesoporous structures, in which the void spaces in the interior and permeable mesopores in the shell are favorable for the reactant and product molecule transports. Our work suggests that yolk–shell structured materials can be used as an innovative and efficient scaffold to encapsulate homogeneous catalysts with the silylation protocol.

## ASSOCIATED CONTENT

### Supporting Information

The following file is available free of charge on the ACS Publications website at DOI: 10.1021/cs5015354.

Hoveyda–Grubbs<sup>2nd</sup> catalyst encapsulation fractions of core–shell structured silica and the completely hollow structured silica, a comparison of TOF over Ru@Y-S and Ru@SBA-1 catalyst for different dienes, recycling results of the Ru complex loaded in yolk–shell structured silica without silylation in RCM, N<sub>2</sub> sorption isotherm and pore size distribution of yolk–shell structured silica (Y-S), TEM images of core–shell structured silica and image of the completely hollow silica, UV/vis absorbance spectra of Hoveyda–Grubbs<sup>2nd</sup> catalyst and diffusion reflectance UV/vis of Y-S (ph) which is only silylated without entrapping Ru complex, <sup>13</sup>C CP-MAS NMR spectrum of the Ru@Y-S catalyst, thermal gravimetric curves of Y-S, Y-S (ph), and Ru@Y-S, kinetic profiles of diethyl diallylmalonate RCM over Hoveyda–Grubbs<sup>2nd</sup> catalyst, Ru@Y-S and Ru@SBA-1 catalysts, and kinetic profiles of diethyl diallylmalonate RCM over the Ru@Y-S catalysts with different shell thicknesses (PDF)

## AUTHOR INFORMATION

### Corresponding Author

\*H.Y.: tel, +86-351-7018371; fax, +86-351-7011688; e-mail, hqyang@sxu.edu.cn.

### Notes

The authors declare no competing financial interest.

## ACKNOWLEDGMENTS

We acknowledge the Natural Science Foundation of China (20903064, 21173137), Program for the Top Young Academic Leaders of Higher Learning Institutions of Shanxi (2011002) and Middle-aged Innovative Talents of Higher Learning Institutions of Shanxi (20120202).

## REFERENCES

- (1) Schrock, R. R. *Angew. Chem., Int. Ed.* **2006**, *45*, 3748–3759.
- (2) Grubbs, R. H. *Angew. Chem., Int. Ed.* **2006**, *45*, 3760–3765.
- (3) Hoveyda, A. H.; Zhugralin, A. R. *Nature* **2007**, *450*, 243–250.
- (4) Schmidt, B.; Geissler, D. *ChemCatChem* **2010**, *2*, 423–429.
- (5) Buchmeiser, M. R. *Chem. Rev.* **2009**, *109*, 303–321.
- (6) Burtscher, D.; Grela, K. *Angew. Chem., Int. Ed.* **2009**, *48*, 442–454.
- (7) Van Berlo, B.; Houthoofd, K.; Sels, B. F.; Jacobs, P. A. *Adv. Synth. Catal.* **2008**, *350*, 1949–1953.
- (8) Liu, G. Y.; He, H. Y.; Wang, J. H. *Adv. Synth. Catal.* **2009**, *351*, 1610–1620.
- (9) Clavier, H.; Grela, K.; Kirschning, A.; Mauduit, M.; Nolan, S. P. *Angew. Chem., Int. Ed.* **2007**, *46*, 6786–6801.
- (10) Lim, J.; Lee, S. S.; Ying, J. Y. *Chem. Commun.* **2010**, *46*, 806–808.
- (11) Bek, D.; Balcar, H.; Zilkova, N.; Zukal, A.; Horacek, M.; Cejka, J. *ACS Catal.* **2011**, *1*, 709–718.
- (12) Marciniak, B.; Rogalski, S.; Potrzebowski, M. J.; Pietraszuk, C. *ChemCatChem* **2011**, *3*, 904–910.
- (13) Bru, M.; Dehn, R.; Teles, J. H.; Deuerlein, S.; Danz, M.; Müller, I. B.; Limbach, M. *Chem. Eur. J.* **2013**, *19*, 11661–11671.
- (14) Cabrera, J.; Padilla, R.; Bru, M.; Lindner, R.; Kageyama, T.; Wilckens, K.; Blof, S. L.; Schanz, H. J.; Dehn, R.; Teles, J. H.; Deuerlein, S.; Müller, K.; Rominger, F.; Limbach, M. *Chem. Eur. J.* **2012**, *18*, 14717–14724.
- (15) Balcar, H.; Čejka, J. *Coord. Chem. Rev.* **2013**, *257*, 3107–3124.
- (16) Zelin, J.; Trasarti, A. F.; Apesteguía, C. R. *Catal. Commun.* **2013**, *42*, 84–88.
- (17) Pastva, J.; Skowerski, K.; Czarnocki, S. J.; Žilková, N.; Čejka, J.; Bastl, Z.; Balcar, H. *ACS Catal.* **2014**, *4*, 3227–3236.
- (18) Staub, H.; Kleitz, F.; Fontaine, F. G. *Microporous Mesoporous Mater.* **2013**, *175*, 170–177.
- (19) Staub, H.; Guillet-Nicolas, R.; Even, N.; Kayser, L.; Kleitz, F.; Fontaine, F. G. *Chem. Eur. J.* **2011**, *17*, 4254–4265.
- (20) Monge-Marcet, A.; Pleixats, R.; Cattoen, X.; Man, M. W. C. *J. Mol. Catal. A: Chem.* **2012**, *357*, 59–66.
- (21) Chen, S. W.; Zhang, Z. C.; Ma, M.; Zhong, C. M.; Lee, S. G. *Org. Lett.* **2014**, *16*, 4969–4971.
- (22) Ferraz, C. P.; Autenrieth, B.; Frey, W.; Buchmeiser, M. R. *ChemCatChem* **2014**, *6*, 191–198.
- (23) Tomasek, J.; Schatz, J. *Green Chem.* **2013**, *15*, 2317–2338.
- (24) Matsugi, M.; Kobayashi, Y.; Suzumura, N.; Tsuchiya, Y.; Shioiri, T. *J. Org. Chem.* **2010**, *75*, 7905–7908.
- (25) Liu, G.; Wang, J. *Angew. Chem., Int. Ed.* **2010**, *49*, 4425–4429.
- (26) Yang, H. Q.; Zhang, L.; Zhong, L.; Yang, Q. H.; Li, C. *Angew. Chem., Int. Ed.* **2007**, *46*, 6861–6865.
- (27) Yang, H. Q.; Zhang, L.; Wang, P.; Yang, Q. H.; Li, C. *Green Chem.* **2009**, *11*, 257–264.
- (28) Bai, S. Y.; Yang, H. Q.; Wang, P.; Gao, J. S.; Li, B.; Yang, Q. H.; Li, C. *Chem. Commun.* **2010**, *46*, 8145–8147.
- (29) Ma, Z. C.; Yang, H. Q.; Qin, Y.; Hao, Y. J.; Li, G. *J. Mol. Catal. A: Chem.* **2010**, *331*, 78–85.
- (30) Hao, Y. J.; Chong, Y. Z.; Li, S. R.; Yang, H. Q. *J. Phys. Chem. C* **2012**, *116*, 6512–6519.
- (31) Yang, H. Q.; Ma, Z. C.; Wang, Y. K.; Wang, Y. W. *Chem. Commun.* **2010**, *46*, 8659–8661.
- (32) Yang, H. Q.; Ma, Z. C.; Zhou, T.; Zhang, W. J.; Chao, J. B.; Qin, Y. *ChemCatChem* **2013**, *5*, 2278–2287.
- (33) Yang, Y.; Liu, J.; Li, X.; Liu, X.; Yang, Q. *Chem. Mater.* **2011**, *23*, 3676–3684.
- (34) Chen, Y.; Chen, H. R.; Shi, J. L. *Acc. Chem. Res.* **2014**, *47*, 125–137.
- (35) Yao, K. X.; Zeng, H. C. *Chem. Mater.* **2012**, *24*, 140–148.
- (36) Zhang, T.; Zhang, Q.; Ge, J.; Goebel, J.; Sun, M.; Yan, Y.; Liu, Y.; Chang, C.; Guo, J.; Yin, Y. *J. Phys. Chem. C* **2009**, *113*, 3168–3175.
- (37) Ha, T. L.; Kim, J. G.; Kim, S. M.; Lee, I. S. *J. Am. Chem. Soc.* **2013**, *135*, 1378–1385.
- (38) Park, J. C.; Bang, J. U.; Lee, J.; Ko, C. H.; Song, H. J. *Mater. Chem.* **2010**, *20*, 1239–1246.
- (39) Pérez-Lorenzo, M.; Vaz, B.; Salgueiriño, V.; Correa-Duarte, M. A. *Chem. Eur. J.* **2013**, *19*, 12196–12211.
- (40) Goebel, J.; Yin, Y. D. *ChemCatChem* **2013**, *5*, 1287–1288.

- (41) Liu, J.; Yang, H. Q.; Kleitz, F.; Chen, Z. G.; Yang, T.; Strounina, E.; Lu, G. Q.; Qiao, S. Z. *Adv. Funct. Mater.* **2012**, *22*, 591–599.
- (42) Fang, X. L.; Liu, Z. H.; Hsieh, M. F.; Chen, M.; Liu, P. X.; Chen, C.; Zheng, N. F. *ACS Nano* **2012**, *6*, 4434–4444.
- (43) Liang, X.; Li, J.; Joo, J. B.; Gutierrez, A.; Tillekaratne, A.; Lee, I.; Yin, Y.; Zaera, F. *Angew. Chem., Int. Ed.* **2012**, *51*, 8034–8036.
- (44) Zhang, Q.; Lee, I.; Joo, J. B.; Zaera, F.; Yin, Y. *Acc. Chem. Res.* **2013**, *46*, 1816–1824.
- (45) Sun, Q.; Guo, C. Z.; Wang, G. H.; Li, W. C.; Bongard, H. J.; Lu, A. H. *Chem. Eur. J.* **2013**, *19*, 6217–6220.
- (46) Shmakov, S. N.; Jia, Y.; Pinkhassik, E. *Chem. Mater.* **2014**, *26*, 1126–1132.
- (47) Shakeri, M.; Roiban, L.; Yazerski, V.; Prieto, G.; Gebbink, R. J. M. K.; Jongh, P. E.; Jong, K. P. *ACS Catal.* **2014**, *4*, 3791–3796.
- (48) Zhang, H.; Jin, R.; Yao, H.; Tang, S.; Zhuang, J.; Liu, G.; Li, H. X. *Chem. Commun.* **2012**, *48*, 7874–7876.
- (49) Stober, W.; Fink, A. *J. Colloid Interface Sci.* **1968**, *26*, 62–69.
- (50) Deng, Y.; Liu, C.; Gu, D.; Yu, T.; Tu, B.; Zhao, D. *J. Mater. Chem.* **2008**, *18*, 91–97.
- (51) Hong, S. H.; Wenzel, A. G.; Salguero, T. T.; Day, M. W.; Grubbs, R. H. *J. Am. Chem. Soc.* **2007**, *129*, 7961–7968.
- (52) Copéret, C.; Basset, J. M. *Adv. Synth. Catal.* **2007**, *349*, 78–92.